Experimental demonstration of the role of local latent heat in Ge pattern formation

Hou Jian-guo
Fujian Institute of Research on the Structure of Matter, Chinese Academy of Sciences, P.O. Box 143, Fuzhou 350 002, Fujian, People's Republic of China

Wu Zi-qin
Center for Fundamental Physics, University of Science and Technology of China, Hefei, Anhui 230 026, People's Republic of China

(Received 19 January 1990)

(Amorphous Ge)/(polycrystalline Au) bilayer thin films with different Au grain size were prepared, and the pattern formation of Ge in annealed films has been investigated. It was found that as the average Au grain size increases from 40 to 410 nm, the Ge patterns change from ramified fractals to simple tip-splitting patterns and finally to round patterns. Furthermore, our experiment proves that the fractal formation in such films is truly dominated by the local-latent-heat, and that the pattern geometry is governed by the latent-temperature field range and the lattice network formed by the grain boundaries of the underlying Au film.

INTRODUCTION

In recent decades, many works have been published about the observation and investigation of nonequilibrium growth in various branches of the sciences, such as dielectric breakdown,[1] electrodeposition,[2,3] Saffman-Taylar viscous-fingering instability,[4,5] irregular crystal growth,[6] and phase transformations in thin solid films.[7–10] All these seemingly unrelated phenomena, except pattern formation in solid films, are well characterized by irreversible pattern formation in a field (electrostatic potential, concentration, pressure, or velocity potential) which satisfies a Laplace equation, and hence is equivalent to the diffusion field, so that the diffusion-limited aggregation (DLA) model[11] is applicable to them. However, nonequilibrium growth in solid films during crystallization is a rather peculiar problem. First, the active field or driven force in such a system is not as easily identified and controlled as those described above. Second, very different patterns formed in different films led to several kinds of descriptions about the growth mechanism. Third, accompanying the diffusion and nucleation, the growth seems to be not fully characterized by the traditional DLA model, in which particles only diffuse and stick to a growing cluster.

In our previous papers,[12,13] the fractal patterns formation in [amorphous Ge (*a*-Ge)]/[polycrystalline Au (poly-Au)], and *a*-Si/*p*-Pd bilayer films were investigated, and the results observed indicated that the fractal morphology is the result of three basic features: (1) heterogeneous nucleation of Ge at Ge/Au interfaces, (2) the growth of Ge crystallites is limited by the grain-boundary diffusion, (3) the local latent heat released by Ge during crystallization may play an important role in the pattern formation. Thus the question arises: Why and how can this short-range field lead to the appearance of ramified patterns that have a fractal geometry on a much larger length scale? What is the relationship between the growth mechanism and the local field?

The purpose of this work is to design an experiment from which we can study the pattern growth more straightforwardly and get a deeper understanding of the growth mechanism in (*a*-Ge)/(poly-Au) systems. From this point of view, several (*a*-Ge)/(poly-Au) films with different grain size of Au were prepared, and pattern formations during crystallization were investigated. Our experimental results indicate that the pattern growth in such films is truly local-latent-heat activated, and that the pattern geometry is governed by the local-latent-temperature field range of Ge and the lattice network formed by the grain boundaries of the underlying Au film.

EXPERIMENT

Specimens were prepared by evaporation on fresh cleavaged NaCl(100) crystal in vacuum with a pressure of 5×10^{-5} Torr. We deposited Au at first and then Ge without breaking the vacuum. The thicknesses of *a*-Ge and poly-Au films are about 20 and 30 nm, respectively. The poly-Au films with different grain size were obtained by changing the evaporation rate or the temperature of the NaCl substrate. Ge was evaporated at the same evaporation rate onto the poly-Au films held at room temperature.

All as-evaporated specimens were annealed in vacuum of about 5×10^{-5} Torr at 150 °C for 1.5 h. After annealing, the specimens were examined by an EM-430 transmission electron microscope (TEM) operated at 300 kV. Quantitative analysis was done by an EDAX-9100 energy-dispersive spectroscopy (EDS) on an H-800 TEM operated at 200 kV. Because of the overlap of the Ge *K* line (9.88 keV) and Au *L* line (9.70 keV), the x-ray intensities of the Ge *L* line (1.19 keV) and Au *M* line (2.14 keV) were used.

RESULTS

(1) *Determination of Au grain size (d_{Au}).* TEM observation shows that the films are homogeneous in morphol-

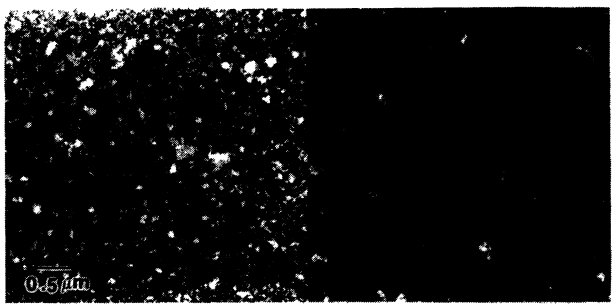

FIG. 1. Bright- and dark-field TEM images of specimen 3 before annealing.

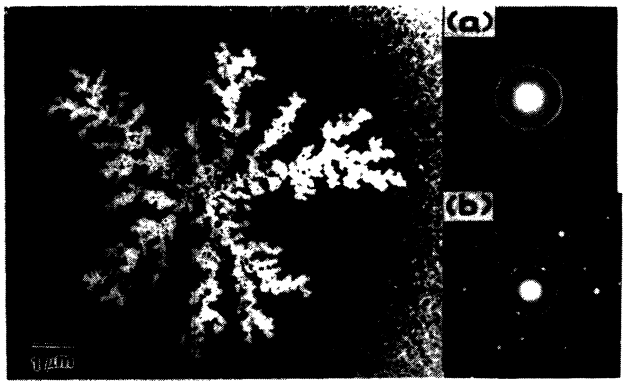

FIG. 2. TEM image and the selected area diffraction patterns of specimen 1 after annealing at 150°C for 1.5 h. Large and bright fractals are formed. (a) The diffraction pattern of the dark region shows no Ge diffraction rings; (b) the diffraction pattern of the fractal region indicates the appearance of small Ge crystallites.

ogy and consist of amorphous Ge and polycrystalline Au before annealing. For each specimen, several dark-field micrographs were taken by use of different parts of the Au(111) diffraction ring. The bright areas in such pictures are those Au crystallites with special rotation. Figure 1 shows the bright- and dark-field micrograph of a specimen. The average values of d_{Au} in different specimens were estimated by measuring the bright areas in dark-field images. The measuring procedure is as follows: for each dark image, we chose ten bright areas at random and have an average value, then d_{Au} is obtained by averaging the values of images with different orientation, and the results are listed in Table I.

(2) *Morphology observation and quantitative analysis.* After annealing at 150°C for 1.5 h, great changes took place in the film morphology. Figure 2 shows the TEM image and the selected-area electron diffraction (SAED) patterns of annealed specimen 1. We can see that large bright DLA-like fractals formed with a size of about 8 μm, and SAED patterns of these bright regions indicate that a-Ge has been crystallized, whereas the SAED patterns of the uniform dark matrix show no Ge diffraction rings. The composition of the dark matrix was determined by EDS to be around $Au_{0.92}Ge_{0.08}$, differing greatly from the average composition of the as-evaporated specimen ($Au_{0.65}Ge_{0.35}$), so we know that almost all Ge atoms aggregate to the fractal regions. Figure 3 shows the pattern growth of specimen 1 at the early annealing stage: small irregular pattern appears with a size of about 100 nm. The picture indicates clearly the branching tendency of the infancy of a Ge pattern. It is obvious that part A is the pattern center, while part B does not seem to grow epitaxially from A. It is reasonable to speculate that B is a new crystallite other than A. In annealed specimen 2, even though these Ge crystalline patterns are thinner and less ramified than that shown in Fig. 2, and their average size is about 4 μm, which is half that of the patterns in specimen 1, they are still DLA-like structures [Fig. 4(a)]. The observation of specimen 2 at early stages reveals a similar result to that shown in Fig. 3.

When the value of d_{Au} is about 150 nm (specimen 3), the shape of Ge patterns is very different from that of specimen 1 and 2 [Fig. 4(b)]. In order to distinguish such less-ramified patterns from those DLA-like patterns, we call them tip-splitting patterns. Figure 4(c) shows that in specimen 4 ($d_{Au}=240$ nm) two kinds of Ge patterns appear in the film morphology: simple tip-splitting pattern (A) and round patterns (B). Further increasing of d_{Au} leads to forming round patterns only, and the diffraction analysis indicates that they are large single-crystal grains [Fig. 4(d)].

From Figs. 2 and 4, we can see clearly how Ge patterns change gradually from well-ramified fractals, in which many small crystallites distributed to nonfractal single-crystal grains, and $d_{Au}=240$ nm is nearly a critical condition in which Ge patterns change from ramified patterns to round ones. Moreover, the average radii of these Ge patterns decrease with the increasing of d_{Au}. Another important result obtained by the TEM observation is that during the annealing, there is no significant change of Au grain size in different specimens.

(3) *Scale-invariant properties of Ge patterns.* TEM images taken of individual patterns were digitized by use of a PDS-101DM microdensitometer at 256×256 resolution. A threshold criterion was then applied to separated pixels in the Ge patterns from those in the background. The quantitative analysis of these digitized images has

TABLE I. Evaporation conditions and grain size of Au films.

	Specimen				
	1	2	3	4	5
Evaporation rate (nm/s)	6	0.1	0.5	0.5	0.5
Substrate temperature (°C)	25	25	150	300	500
Grain size (nm)	40±5	75±11	150±15	240±17	410±30

FIG. 3. TEM image shows the fractal morphology at the early growth stage (annealing time is about 15 min); part A is an original growth center, while part B is a new crystallite other than A.

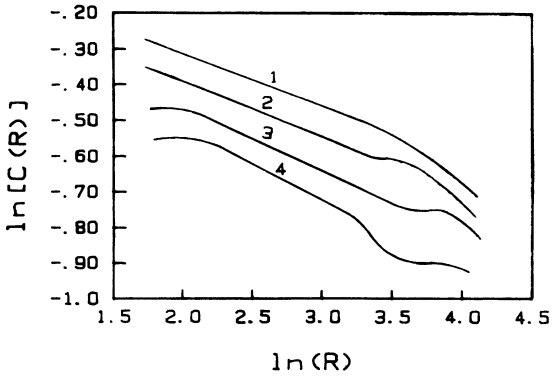

FIG. 5. Curves of the logarithmic density-density correlation function vs radius. The numbers denote the curve of the different specimens. It can be found that linear ranges decrease with the increase of d_{Au}.

been carried out by the density-density correlation function method.[11] It is found that for specimens 1–4, their correlation functions behave as a power law $[C(R)\sim R^{-a}]$ when R lies in certain ranges (Fig. 5). Therefore in a limited range, they are self-similar. Figure 6 shows the relationship between the relative liner range $\Delta R/R_g$ and d_{Au} (where R_g is the average radius of gyration). We find that for specimens 1 and 2, $\Delta R/R_g$ keeps a constant, and its value is equivalent to those DLA's.[11] Therefore, the patterns shown in Figs. 2 and 4(a) are fractals, and the fractal dimensions determined from the $\ln(R)\sim\ln[C(R)]$ curves are 1.70±0.01 and 1.68±0.03, respectively, while for specimens 3 and 4, $\Delta R/R_g$ decreases remarkably with the increasing of d_{Au}. Although limited liner ranges exist in the $\ln(R)\sim\ln[C(R)]$ curves, the ramified patterns shown in Figs. 4(b) and 4(c) can hardly be considered as fractals because $\Delta R/R_g$ is too small. Therefore, according to the characteristic of $C(R)$, the pattern formations can be divided into three regimes: (1) the fractal growth regime, in which correlation length is nearly a constant ($\sim 0.4R_g$) and the fractal dimension decreases with the increase of d_{Au}, (2) the simple-splitting growth regime, in which correlation length decreases remarkably with the increase of d_{Au}, and (3) the round growth regime, in which only solid patterns are formed (Fig. 6).

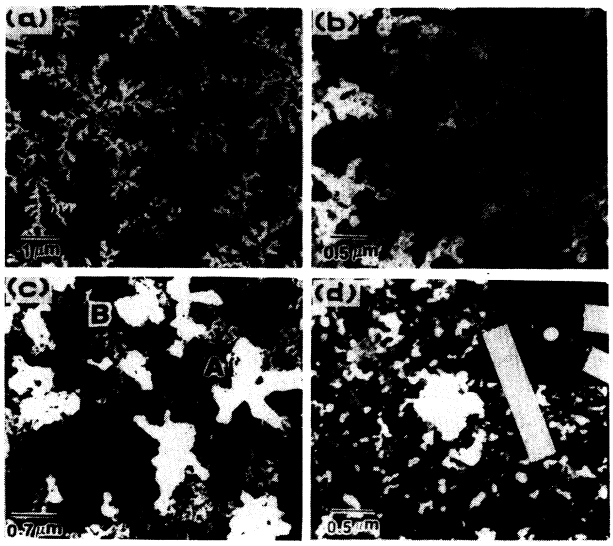

FIG. 4. TEM images of the specimens with different grain size of Au after annealing at 150 °C for 1.5 h. We can see clearly how bright crystalline Ge regions change gradually from well-ramified patterns to round patterns: (a) specimen 2; (b) specimen 3; (c) specimen 4; and (d) specimen 5. The bright spots in the SAED pattern (see above) indicate that the round Ge region is a large single-crystal grain.

DISCUSSION

It is known that[14,15] the basic features of metal-enhanced crystallization in (a-Ge)/(poly-Au) system are (1) heterogeneous nucleation of Ge in energy favorite sites at Ge/Au interfaces (such as the triple points of the grain boundary of Au film) and, (2) crystallite growth is

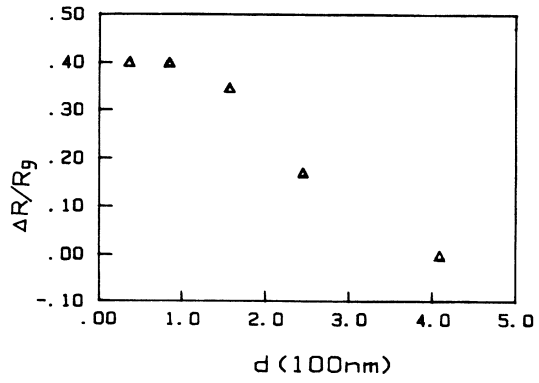

FIG. 6. Plot of the relative linear range ($\Delta R/R_g$) vs the average grain size of Au (d_{Au}), where R_g is the radius of gyration, and the data of specimen 4 are obtained by averaging over those ramified patterns.

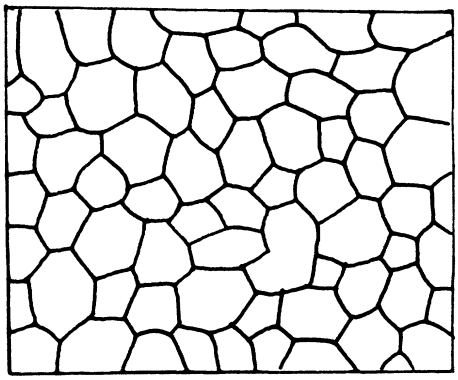

FIG. 7. Schematic projection of the Au grain-boundary network and the triple grain-boundary points of poly-Au films.

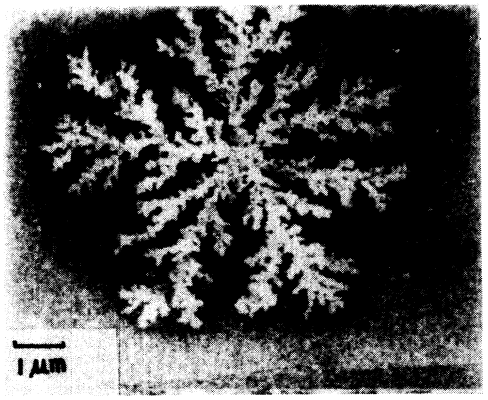

FIG. 8. TEM image shows the growing Ge pattern surrounded by a narrow Au-rich region in which atomic diffusion and nucleation take place.

limited by the grain-boundary diffusion because the less-dense packing of atoms at the grain boundary leads to a greater atomic mobility. Figure 7 shows the schematic projection of the Au grain-boundary network and the triple grain boundary points; with different length scales, the projection can adapt to specimens with different d_{Au}, so that Au films provided a matrix in which Ge can nucleate and diffuse easily.

Now according to the careful observations at the early growth stage (see Fig. 3 and lattice images presented in our previous paper[13]), we can get a picture of the microscopic model for the growth. At the beginning of crystallization, a primary nucleus caused by thermal fluctuation appears in the favorite site, and then the growth of the nucleus becomes boundary diffusion limited; at the same time, the released latent heat of crystallization leads to a rise in temperature in surrounding regions and may stimulate new nuclei to appear at its boundary for further diffusion-limited growth; this is the so-called "random successive nucleation (RSN)" process, and the progressive screening of a given Ge crystallite by the new stimulated nucleus at its boundary limits its own growth; it is obvious that the Ge pattern must grow along the grain-boundary network when the RSN process takes place. Although the microscopic growth mechanism described above enables us to understand the polycrystalline and the branching natures of the Ge pattern, there are two problems which need further discussion. That is why large fractals cannot form in those specimens with a larger grain-boundary network and why fractal patterns in specimens 1 and 2 are so analogous to the traditional DLA patterns that formed only by particle diffusion.

As shown in Fig. 8, between a growing Ge pattern and the amorphous Ge matrix, there is a narrow dark Au-rich region indicating the occurrence of atomic diffusion. This means that Ge atoms should move a certain distance before they reach the growth zone near the Ge/Au boundary. For detailed discussion, we introduce two length scales associated with the diffusion and nucleation processes: one is the average effective range of local temperature field (L) in which latent heat has sufficient energy to promote Ge atoms to overcome the diffusion barrier, and the other is the lattice constant (D) of the grain-boundary network formed by the underlying Au film. The value of D is naively considered to be the same order of d_{Au}, i.e., $D \approx d_{Au}$, while the value of L can be approximately estimated by measuring the width between the tip of the branch and the amorphous matrix. Although the width of the different specimen or the same specimen at a different annealing stage varied slightly, its dominant value, obtained by averaging over several patterns, is about 263 ± 50 nm. This result is expected because the latent heat of crystallization is a constant. Approximately we let $L \approx 260$ nm.

Qualitatively, $L/D > 1$ means that Ge atoms should diffuse following a random path along the grain-boundary network shown in Fig. 7, and that RSN processes will happen during annealing. As a result, the ramified patterns with small Ge crystallites will grow along grain boundaries. Therefore we can speculate that even though nucleation plays an important role in the pattern formations of these specimens, the location of new nuclei at the Ge/Au boundary is actually determined by the atomic diffusion along the Au grain-boundary network. It is obvious that the larger the value of L/D is, the more the boundary diffusion process in Ge/Au systems is similar to that of the traditional DLA model, in which particles diffuse on a two-dimensional lattice. Therefore, DLA-like patterns can form in specimens 1 and 2 ($L/D > 3.5$). Conversely, in specimen 5 ($L/D < 1$), no stimulated nuclei appear and the Ge crystallites grow independently; as a result, large single-crystal grains appear in the film morphology. $L/D \approx 1$ is the intermediate case (specimen 4) in which both kinds of patterns formed randomly.

In summary, we conclude that the pattern formation in a-Ge/Au systems is truly dominated by the local temperature field, so that it is a kind of self-activated random-growth phenomenon, and the correlation property of the Ge pattern is determined by the local-latent-heat field range and the grain-boundary network formed by the underlying polycrystalline Au film.

[1]L. Niemeyer, L. Pietronero, and H. T. Wiesmann, Phys. Rev. Lett. **52**, 1033 (1984).
[2]R. Brady and R. Ball, Nature (London) **309**, 225 (1984).
[3]M. Matsushita, M. Sano, Y. Hayakana, H. Honjo, and Y. Sawada, Phys. Rev. Lett. **53**, 286 (1984).
[4]L. Parerson, Phys. Rev. Lett. **52**, 1621 (1984).
[5]J. Nittmann, G. Daccord, and H. E. Stanly, Nature (London) **314**, 141 (1985).
[6]H. Honjo, S. Ohta, and M. Mastushita, J. Phys. Soc. Jpn. **55**, 2487 (1986).
[7]W. T. Elam, S. A. Wolf, J. Sprague, D. U. Gubser, D. van Vechten, G. L. Braz, Jr., and P. Meakin, Phys. Rev. Lett. **54**, 701 (1987).
[8]B. X. Liu, L. J. Huang, K. Tao, C. H. Shang, and H. D. Li, Phys. Rev. Lett. **59**, 75 (1987).
[9]Gy. Radnoczi, T. Vicsek, L. M. Sander, and D. Grier, Phys. Rev. A **35**, 4012 (1987).
[10]G. Deutscher and Y. Lareah, Phys. Rev. Lett. **60**, 1510 (1988).
[11]T. A. Witten and L. M. Sander, Phys. Rev. Lett. **47**, 1400 (1980); Phys. Rev. B **27**, 5686 (1983).
[12]Duan Jian-zhong and Wu Zi-qin, Solid State Commun. **64**, 1 (1987).
[13]Hou Jian-guo and Wu Zi-qin, Phys. Rev. B **40**, 1008 (1989).
[14]C. C. Tsai, J. Vac. Sci. Technol. **21**(2), 632 (1982).
[15]Zhang Ren-ji and Wu Zi-qin, Acta Phys. Sin. **35**, 365 (1986).

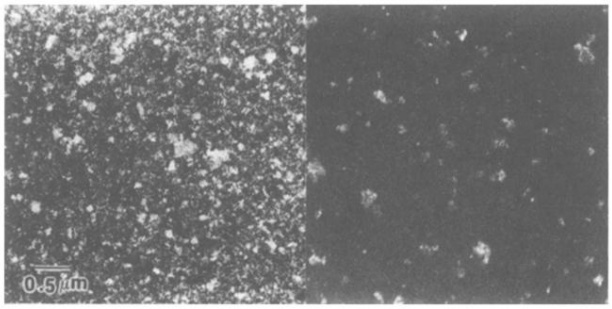

FIG. 1. Bright- and dark-field TEM images of specimen 3 before annealing.

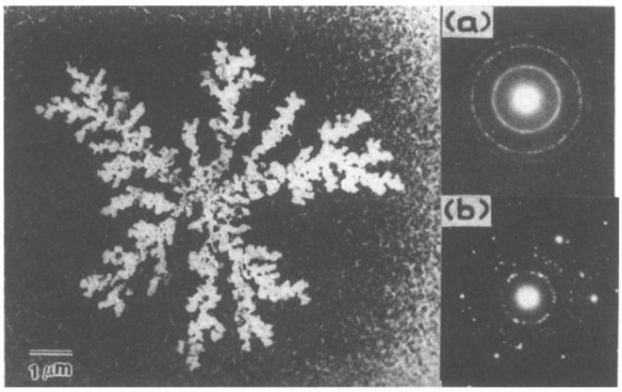

FIG. 2. TEM image and the selected area diffraction patterns of specimen 1 after annealing at 150 °C for 1.5 h. Large and bright fractals are formed. (a) The diffraction pattern of the dark region shows no Ge diffraction rings; (b) the diffraction pattern of the fractal region indicates the appearance of small Ge crystallites.

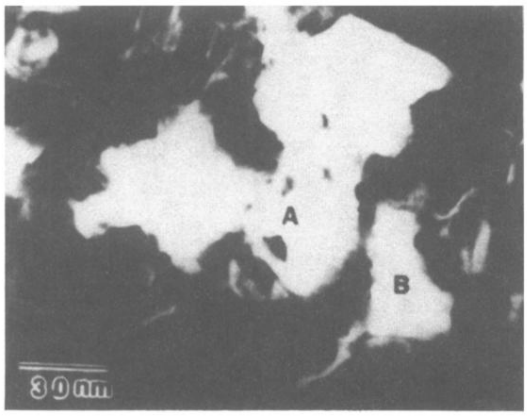

FIG. 3. TEM image shows the fractal morphology at the early growth stage (annealing time is about 15 min); part *A* is an original growth center, while part *B* is a new crystallite other than *A*.

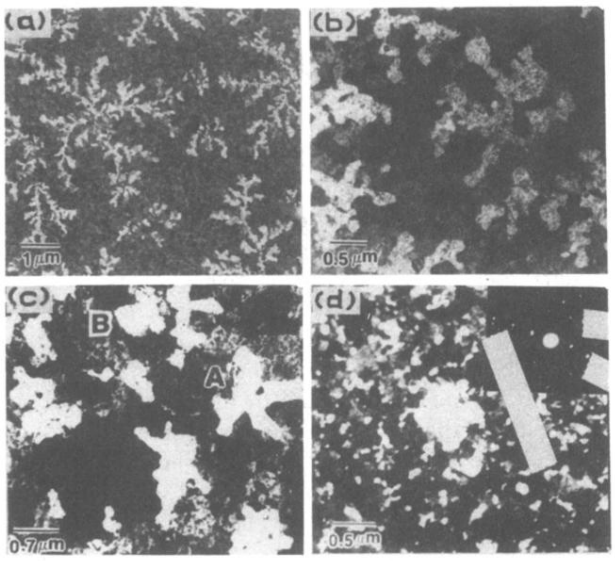

FIG. 4. TEM images of the specimens with different grain size of Au after annealing at 150 °C for 1.5 h. We can see clearly how bright crystalline Ge regions change gradually from well-ramified patterns to round patterns: (a) specimen 2; (b) specimen 3; (c) specimen 4; and (d) specimen 5. The bright spots in the SAED pattern (see above) indicate that the round Ge region is a large single-crystal grain.

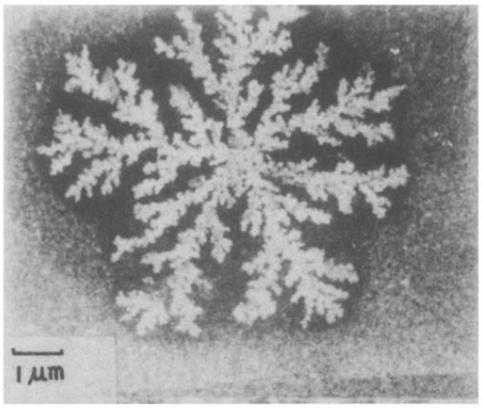

FIG. 8. TEM image shows the growing Ge pattern surrounded by a narrow Au-rich region in which atomic diffusion and nucleation take place.